

Roles of STAT3/SOCS3 Pathway in Regulating the Visual Function and Ubiquitin-Proteasome-dependent Degradation of Rhodopsin during Retinal Inflammation*

Received for publication, March 20, 2008, and in revised form, June 20, 2008 Published, JBC Papers in Press, July 9, 2008, DOI 10.1074/jbc.M802238200

Yoko Ozawa^{‡§}, Keiko Nakao^{§¶}, Toshihide Kurihara^{‡§}, Takuya Shimazaki[§], Shigeto Shimmura[‡], Susumu Ishida[‡], Akihiko Yoshimura^{||**}, Kazuo Tsubota[‡], and Hideyuki Okano^{§###\$1}

From the Departments of [‡]Ophthalmology and [§]Physiology, Keio University School of Medicine, Tokyo 160-8582, Japan, [¶]Department of Physiology, Faculty of Medicine, Saitama Medical University, Saitama 350-0495, Japan, ^{||}Department of Microbiology and Immunology, Keio University School of Medicine, Tokyo 160-8582, Japan, ^{**}Division of Molecular and Cellular Immunology, Medical Institute of Bioregulation, Kyushu University, Fukuoka 812-8582, Japan, and ^{##}Core Research for Evolutional Science and Technology (CREST) and ^{\$}Solution Oriented Research for Science and Technology (SORST), Japan Science and Technology Corporation (JST), Saitama 332-0012, Japan

Inflammatory cytokines cause tissue dysfunction. We previously reported that retinal inflammation down-regulates rhodopsin expression and impairs visual function by an unknown mechanism. Here, we demonstrate that rhodopsin levels were preserved by suppressor of cytokine signaling 3 (SOCS3), a negative feedback regulator of STAT3 activation. SOCS3 was expressed mainly in photoreceptor cells in the retina. In the SOCS3-deficient retinas, rhodopsin protein levels dropped sooner, and the reduction was more profound than in the wild type. Visual dysfunction, measured by electroretinogram, was prolonged in retina-specific SOCS3 conditional knockout mice. Visual dysfunction and decreased rhodopsin levels both correlated with increased STAT3 activation enhanced by SOCS3 deficiency. Interleukin 6, one of the inflammatory cytokines found during retinal inflammation, activated STAT3 and decreased rhodopsin protein in adult retinal explants. This was enhanced by inhibiting SOCS3 function *in vitro*, indicating that rhodopsin reduction was not a secondary effect in the mutant mice. Interestingly, in the inflamed SOCS3-deficient adult retina, rhodopsin decreased post-transcriptionally at least partly through ubiquitin-proteasome-dependent degradation accelerated by STAT3 activation and not transcriptionally as in the developing retina, on which we reported previously. A STAT3-dependent E3 ubiquitin ligase, Ubr1, was responsible for rhodopsin degradation and was up-regulated in the inflamed SOCS3-deficient retinas. These results indicate that in wild-type animals, a decrease in rhodopsin during inflammation is minimized by endogenous SOCS3. However, when STAT3 activation exceeds some threshold beyond the compensatory activity of endogenous SOCS3, rhodopsin levels decrease. These findings suggest

SOCS3 as a potential therapeutic target molecule for protecting photoreceptor cell function during inflammation.

Signals from inflammatory cytokines such as interleukin 6 (IL-6)² signal through the gp130 receptor and cause tissue dysfunction in various organs, including the intestine (1), joints (2), and retina (3, 4). One effect of retinal inflammation that impairs visual function is the decreased expression of rhodopsin, an essential protein for photoreceptor function (4), but the mechanism of this down-regulation has not been elucidated.

Previous reports have shown that gp130 signals influence rhodopsin expression in the developing retina. The ciliary neurotrophic factor (CNTF) signal through gp130 inhibits rhodopsin expression (5–7) via STAT3 activation in the perinatal period (8, 9). The high level of STAT3 activation in the late embryonic period must be down-regulated postnatally to initiate rhodopsin expression and photoreceptor cell differentiation (8). STAT3 activation is declined not only by cytokine depletion but also by suppressor of cytokine signaling 3 (SOCS3), a negative feedback modulator of STAT3 activation (10). SOCS3 functions by inhibiting the Janus kinase (JAK), which activates STAT3 downstream of the gp130 signal. Because the inhibition of STAT3 permits the transcription of *rhodopsin* and its upstream transcription factor *crx* during development (8, 10), it seemed likely that a similar mechanism might be responsible for inhibiting rhodopsin expression during inflammation.

If rhodopsin expression during inflammation was indeed negatively regulated by STAT3 activation and rescued by SOCS3, SOCS3 would be an ideal therapeutic target molecule. In fact, CNTF promotes retinal survival in degenerative disease models but does not improve electroretinogram (ERG),

* This study was supported by a grant-in-aid from the Ministry of Education, Science, and Culture (MEXT) of Japan (to Y. O., K. T., and H. O.), a grant from SORST, the Japan Society for Promotion of Science (to H. O.), and the 21st Century COE program of MEXT (to Keio University). The costs of publication of this article were defrayed in part by the payment of page charges. This article must therefore be hereby marked "advertisement" in accordance with 18 U.S.C. Section 1734 solely to indicate this fact.

Author's Choice—Final version full access.

¹ To whom correspondence should be addressed: 35 Shinanomachi, Shinjuku-ku, Tokyo 160-8582, Japan. Tel.: 81-3-5363-3747; Fax: 81-3-3357-5445; E-mail: hidokano@sc.itc.keio.ac.jp.

² The abbreviations used are: IL, interleukin; CNTF, ciliary neurotrophic factor; SOCS, suppressor of cytokine signaling; ERK, extracellular signal-regulated kinase; JAK, Janus kinase; STAT, signal transducers and activators of transcription; UPS, ubiquitin-proteasome system; EGFP, enhanced green fluorescent protein; ERG, electroretinogram; LPS, lipopolysaccharide; RT, reverse transcription; shRNA, small hairpin RNA; E2, ubiquitin carrier protein; E3, ubiquitin-protein isopeptide ligase; ONL, outer nuclear layer; OS, outer segment; WT, wild-type mice; KO, α -Cre SOCS3^{lox/lox} knock-out mice.

SOCS3 Preserves Rhodopsin Expression and Visual Function

because rhodopsin expression is decreased by unknown mechanisms (11, 12). This side effect is now the focus of considerable interest, as CNTF is a potential candidate for the treatment of retinitis pigmentosa (11–13). If SOCS3 preserves rhodopsin levels, it might be a useful adjunct therapy with CNTF.

Here, we have demonstrated that SOCS3 preserved rhodopsin levels and visual function by reducing STAT3 activation during retinal inflammation. We used a model of LPS-induced retinitis with uveitis in which the IL-6/gp130 receptor signal is up-regulated (3) and rhodopsin is down-regulated (4). During retinal inflammation, SOCS3-deficient mice showed excessive STAT3 activation, which caused a more profound loss of rhodopsin and worse visual disturbance than identically stimulated wild-type animals. Furthermore, the endogenous SOCS3 in wild-type mice contributed to the recovery of visual function but failed to prevent the effects of activated STAT3 at its peak levels. The reduced rhodopsin levels were regulated post-transcriptionally, unlike in embryos, by degradation through the ubiquitin-proteasome system (UPS) most probably mediated by the STAT3-dependent E3 ubiquitin ligase, Ubr1. Thus, SOCS3 was required to minimize the influence of inflammatory cytokines and preserve visual function. SOCS3 therefore may be a good therapeutic target for controlling retinal neural function during inflammation.

EXPERIMENTAL PROCEDURES

Animals—C57BL/6 mice (8 weeks old) were purchased from Clea Japan (Tokyo). SOCS3 floxed mice were generated in Dr. Yoshimura's laboratory (Kyushu University) (14), and α -Cre transgenic mice were generously provided by Dr. P. Gruss (Max Planck Institute) (15). Animals received a single intraperitoneal injection of *Escherichia coli* lipopolysaccharide (LPS) (6.0 mg/kg body weight) (Sigma) in phosphate-buffered saline. Animals were sacrificed and evaluated at the indicated time points. CAG-CAT-EGFP transgenic mice, which were used to show the expression of Cre recombinase, were kindly provided by Dr. J. Miyazaki (Osaka University) (16). All procedures conformed to the Policies on the Use of Animals and Humans in Neuroscience Research as approved by the Institutional Safety Committee on Recombinant DNA Experiments and the Animal Research Committee of Keio University.

Retinal Explant Culture—Retinal explant culture was performed using adult mouse neural retina as described previously, with modifications to the protocol described by Tomita *et al.* (17). Briefly, eyes were enucleated, and the neural retinas were isolated and placed on a Millicell chamber filter (Millipore, Billerica, MA; pore size, 0.4 μ m) with the ganglion cell layer facing up. The chamber was then placed in a well of a 6-well culture plate that contained 50% minimum Eagle's medium (Invitrogen), 25% Hanks' balanced salt solution (Invitrogen), 25% horse serum (Thermo Trace, Victoria, Australia), 200 mM L-glutamine, and 6.75 mg/ml D-glucose. The explants were incubated at 34 °C in 5% CO₂ for 1 night and then at 37 °C in 5% CO₂ for 4 h in Dulbecco's modified Eagle's medium (Invitrogen) containing 0.5% fetal bovine serum with or without IL-6 (10 ng/ml, Peprotech, Rocky Hill, NJ), AG490 (7.5 or 15 μ M, Calbiochem), or MG132 (10 μ M, Biomol, Philadelphia). For

immunoprecipitation, adult retinal explants were incubated for 30 min under each condition with MG132 (10 μ M).

Electroporation—Electroporation was performed as described previously (8, 10). Briefly, a retinal explant on a filter membrane was placed into the appropriate DNA solution (5 μ g/ μ l in phosphate-buffered saline minus), which was dropped on an agarose gel, and electric pulses (20 V for 50 ms, 6 times) were applied with an electroporator (CUY21 NEPPA GENE, Chiba, Japan) without contacting the tissue. Retinas were transfected with an expression vector carrying the cDNA for human SOCS3 (prepared in Dr. Yoshimura's laboratory, Kyushu University) (18, 19) or Cre recombinase under the control of the CAG promoter (generously provided by Dr. H. Niwa, Kumamoto University) (16) along with pCAG-EGFP (an expression vector containing EGFP (10:1)). The control was an empty transfection vector, pCAG, which was introduced along with pCAG-EGFP.

Lentivirus Infection—Lentivirus vector carrying shRNA targeting Ubr1 and a random control shRNA was purchased from Sigma. Lentivirus was produced along with the company's guidance and infected into adult retinal explants.

Immunohistochemistry—Cryosections of the retina (12–16 μ m) fixed with 4% paraformaldehyde were prepared as described elsewhere (8). The sections were first incubated with 0.1% Triton and 10% goat serum in phosphate-buffered saline and then at 4 °C with primary mouse anti-rhodopsin (1:100, Abcam, Cambridge, MA), rabbit anti-rhodopsin (1:1000, LSL, Tokyo), or anti-glutamine synthetase antibodies (1:400, BD Biosciences, San Jose, CA) diluted in 0.1% Triton and 2% goat serum. The sections were then incubated with Alexa 555-conjugated goat anti-mouse or anti-rabbit IgG antibody (1:500, Molecular Probes; Invitrogen). For immunostaining with rabbit anti-phospho-STAT3 (Tyr-705) (1:50, Cell Signaling Technology, Danvers, MA), rabbit anti-phospho-ERK (1:50, Cell Signaling Technology), and rabbit anti-SOCS3 (1:100, anti-SOCS3 C terminus, generated in Dr. Yoshimura's Laboratory at Kyushu University) (10, 14, 20) antibodies and mouse anti-Ubr1 antibody (1:100, Abnova, Taiwan), the sections were preincubated at 100 °C for 5 min in tissue retrieval solution (TRS 1699, Sigma) and then incubated at 4 °C overnight with primary antibody diluted in blocking agent with 0.3 or 0.1% Triton. Finally, the immunoreactions were detected with a tyramide signal amplification fluorescein system (PerkinElmer Life Sciences), as described previously (8). Double immunostained sections were examined with a laser scanning confocal microscope (LSM510, Carl Zeiss). Each set of experiments was performed in parallel. The length of the outer segments was measured in the mid-peripheral part of the retinas in three sections from three individual animals after immunostaining with anti-rhodopsin antibody.

Immunoblot Analysis—Retinal extract proteins were fractionated by electrophoresis on SDS-polyacrylamide gels and then electrophoretically transferred to membranes and incubated with rabbit anti-phospho-STAT3 (Tyr-705) (1:1000, Cell Signaling Technology), rabbit anti-rhodopsin (1:16000, LSL), mouse anti-rhodopsin (1:1000, Abcam), rabbit anti-Ubr1 (1:200, Abcam), mouse anti- α -tubulin (1:2000, Sigma), or mouse anti-ubiquitin (1:500, Nippon Biotest Laboratories, Tokyo) antibodies followed by horseradish peroxidase- or bio-

tin-conjugated secondary antibodies (Jackson Immuno-Research Laboratory, West Grove, PA). The immunoreactive proteins were detected with an ECL system (Amersham Biosciences). The intensity of the bands was measured using the NIH Imaging system, and the levels of proteins of interest were normalized to that of α -tubulin. Rhodopsin appeared as two bands on the immunoblots, which probably represent monomeric and dimeric forms. These bands appeared in all of the samples (as the intensity levels of the bands in each sample were in parallel, we have shown only the monomers in most of the figures for the sake of simplicity). For immunoprecipitation, retinal extract was obtained in the presence of MG132 (20 μ M) in the lysis buffer and reacted with rabbit anti-rhodopsin.

Real-time RT-PCR—Total RNA was extracted from the retina, and the cDNAs were synthesized after RNase-free DNase (Invitrogen) treatment. Real-time PCR was performed using an Mx3000p, with SYBR Green (Takara Bio, Shiga, Japan). The primers for *crx* and *rhodopsin* detection were described by Furukawa *et al.* (21) and Peng *et al.* (22), respectively. The results are presented as the ratio of the mRNA of interest to the mRNA of an internal control gene, *gapdh*. The *gapdh* primer sequences were accacagtccatgc-catcac (forward) and tccaccaccctgttgctgta (reverse).

Electroretinogram—ERG recording was performed as described previously (4, 23). Briefly, animals were dark-adapted for at least 12 h and prepared under dim red illumination. Mice were anesthetized with pentobarbital sodium (70 mg/kg of body weight; Dainippon Sumitomo Pharmaceutical Co., Osaka, Japan) and kept on a heating pad throughout the experiment. The pupils were dilated with one drop of a mixed solution of 0.5% tropicamide and 0.5% phenylephrine (Santen Pharmaceutical Co., Osaka, Japan). The ground electrode was a subcutaneous needle inserted in the tail, and the reference electrode was placed subcutaneously between the eyes. The active contact lens electrodes (Mayo, Inazawa, Japan) were placed on the cornea. Recordings were performed with the PowerLab system 2/25 (AD Instruments, New South Wales, Australia). Responses were differentially amplified and filtered through a digital bandpass filter ranging from 0.3 to 500 Hz to yield a- and b-waves. Light pulses of 800 cd-s/m² were delivered via a Ganzfeld System SG-2002 (LKC Technologies). The amplitude of the a-wave was measured from the base line to the trough of the a-wave, and the amplitude of the b-wave was determined from the trough of the a-wave to the peak of the b-wave. The implicit time of the a- and b-waves was measured from the onset of stimulus to the peak of each wave.

Statistical Analysis—Data were expressed as the mean \pm S.D. Statistical significance was tested with the unpaired two-tailed Student's *t* test or analysis of variance.

RESULTS

Expression of SOCS3 and Activated STAT3 during Inflammation in the Retina—First, we found that SOCS3, which is expressed mainly in the photoreceptor cells during development (10), was also expressed in the photoreceptor cells in the normal adult retinas, most prominently in the inner segments (Fig. 1A). SOCS3 was present in the neurites of the cells in the inner layers as well. Eight hours after LPS injection, which induces retinal inflammation (3, 4, 24), SOCS3 was clearly

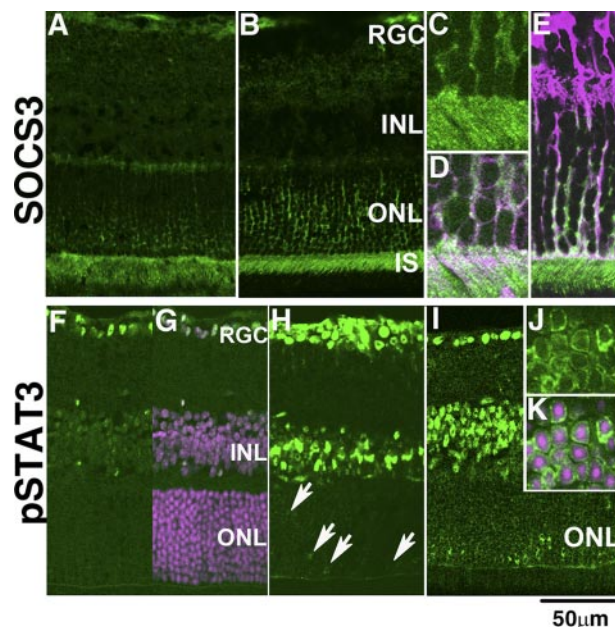


FIGURE 1. Expression of SOCS3 and activated STAT3 during retinal inflammation. Expression of SOCS3 in the adult retinas under control condition (A) and 8 h after LPS injection (B–E) was analyzed by immunohistochemistry. Magnified views of the ONL and inner segments (IS) after LPS injection are shown in C and D (SOCS3, green; rhodopsin, pink; merged image is shown in D). Müller glial cells after LPS injection are also shown in E (SOCS3, green; glutamine synthetase, pink; merged image). STAT3 activation was detected by an anti-phosphoSTAT3 antibody under control conditions (F and G) (phospho-STAT3, green; nuclei counter stained with Hoechst, pink; merged image is shown in G) and at 8 h (H, arrows) and 16 h (I–K) after LPS injection. Higher magnifications of ONL cells (J and K) (phospho-STAT3, green; nuclei counter-stained with Hoechst, pink; merged image is shown in K). RGC, retinal ganglion cells; INL, inner nuclear layer.

observed not only in the inner segments (IS) but also in the cell bodies of the photoreceptor cells in the outer nuclear layer (ONL) (Fig. 1, B–D), as well as in the Müller glial cells recognized by immunostaining for anti-glutamine synthetase (Fig. 1E). This is consistent with the fact that SOCS3 is rapidly up-regulated during LPS-induced inflammation in certain organs and tissues (2, 25–28).

We had reported previously immunoblot evidence that STAT3, which is activated downstream in IL-6/gp130 signaling, is also activated in LPS-induced retinal inflammation (4). In the present study, we used immunohistochemistry to learn which cells express activated STAT3. In the control retina, we detected activated STAT3 in retinal ganglion cells (RGC) and some of the inner nuclear layer cells (INL) in their nuclei (Fig. 1, F and G) but not in the photoreceptor cells (Fig. 1F). Eight hours after LPS injection, activated STAT3 was up-regulated in the retinal ganglion and inner nuclear layer cells, and moreover, activated STAT3 appeared in a subset of photoreceptor cells as well (Fig. 1H, arrows). Sixteen hours after LPS injection, activated STAT3 was obvious in most of the photoreceptor cells in the ONL (Fig. 1I). Thus, STAT3 activation was gradually, not rapidly, up-regulated in the photoreceptor cells by 16 h after LPS administration. In the photoreceptor cells, activated STAT3 (Fig. 1, J and K, green) was observed mainly in the cytoplasm with slight expression in the nuclei (Fig. 1K, pink). Generally, STAT3 is transported into the nucleus as soon as it is phosphorylated, where it up-regulates the transcription of its

SOCS3 Preserves Rhodopsin Expression and Visual Function

target genes (29). However, some cytosolic phosphorylated form of STAT3 activated by the IL-6/gp130 signal has been found in the endosomal fraction as well, which then translocates into the nucleus and activates transcription (29–31). The activated STAT3 in the photoreceptor cells may have different kinetics from that in the retinal ganglion and inner nuclear layer cells, but it may also act as a transcription regulator in both cases. As regards activated ERK, another pathway downstream of IL-6/gp130 signaling, it was observed mainly in the cells of the inner layers, and hardly any was detected in the photoreceptor cells (data not shown).

Down-regulation of Rhodopsin Is More Severe and ERG Changes More Prolonged in SOCS3-deficient Mice after LPS Injection—Previous findings had suggested the correlation between STAT3 activation and down-regulation of rhodopsin protein during retinal inflammation (4). If this was correct, it seemed likely that SOCS3 inhibited STAT3 activation in the photoreceptor cells to avoid the decrease in rhodopsin. To investigate this possibility, we obtained mice with a SOCS3-deficient retina by generating retinal-specific conditional knock-out mice (α -Cre $SOCS3^{lox/lox}$ mice), because the total knock-out mutation in mice is embryonic lethal (32). The α -Cre recombinase is expressed only in the retina; its expression begins at embryonic day 12 (15) and extends from the mid-peripheral to the peripheral retina, including the photoreceptor cells at birth (8, 10). In α -Cre $SOCS3^{lox/lox}$ mice, SOCS3 was deleted in these areas of the retina, and rod photoreceptor cell differentiation was delayed at postnatal day 3, but the differentiation caught up with wild type by adulthood (10). The α -Cre-mediated recombination of the SOCS3 gene in these areas of the adult retina was confirmed, using α -Cre CAG-CAT-EGFP transgenic mice (data not shown).

We analyzed the level of rhodopsin protein, an essential protein for visual function, in the inflamed adult retinas. The level was unchanged in the α -Cre $SOCS3^{lox/lox}$ mice under control conditions (Fig. 2, A and D). However, 8 h after LPS injection, the rhodopsin level in the α -Cre $SOCS3^{lox/lox}$ mice had markedly decreased to 50% of that in the LPS-administered wild-type mice, which still showed base-line rhodopsin levels (Fig. 2, A and D). Then, 48 h after the LPS injection, the rhodopsin level was decreased to 40% of the control in the wild-type mice and 20% of the control in the α -Cre $SOCS3^{lox/lox}$ mice (Fig. 2, A and D). Thus, the decrease in rhodopsin level after LPS injection was more severe in the α -Cre $SOCS3^{lox/lox}$ mice.

We further compared the morphological change in the photoreceptor cells during inflammation. Rhodopsin is located mainly in the outer segments (OS) of the photoreceptor cells. The OS are composed of discs in which photons are captured and transduced by rhodopsin. If rhodopsin were to run out during inflammation, the OS should be shorter than in the controls, which might affect visual function. Indeed, the length of the OS was shorter 48 h after LPS injection even in wild-type mice compared with controls, but the reduction in OS length was twice as great in the LPS-administered α -Cre $SOCS3^{lox/lox}$ mice (Fig. 2, B, C, and E). This reduction in OS length was consistent with the amount of rhodopsin that remained during inflammation.

To learn how SOCS3 influences the visual dysfunction caused by inflammation, we recorded ERG responses in wild-

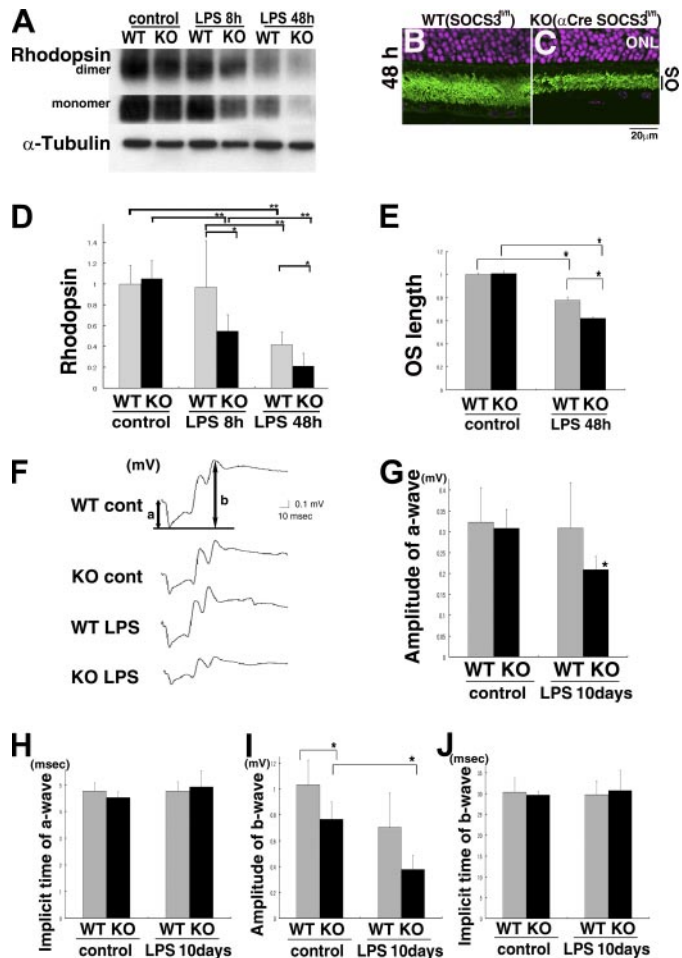


FIGURE 2. Decrease in rhodopsin protein and ERG changes during retinal inflammation were more severe in the SOCS3-deficient mice. Rhodopsin levels in wild-type and α -Cre $SOCS3^{lox/lox}$ mice under control conditions and after LPS injection were measured by immunoblot analysis with anti-rhodopsin antibody normalized to α -tubulin (A and D). Levels of rhodopsin monomer and dimer were parallel under all conditions. $n = 5, 5, 7, 7, 5,$ and 4 for WT control, KO control, WT 8 h, KO 8 h, WT 48 h, and KO 48 h, respectively. The length of OS was measured in the mid-peripheral part of the retina under control condition and 48 h after LPS injection (B, C, and E: rhodopsin, green; Hoechst representing nuclei in ONL, pink). ERG responses from wild-type and SOCS3-deficient mice under control condition and 10 days after LPS injection (F–J). $n = 5, 5, 4,$ and 4 for WT control, KO control, WT 10 days, and KO 10 days, respectively. Data are expressed as the mean \pm S.D. *, $p < 0.05$; **, $p < 0.01$; a, a-wave; b, b-wave.

type and α -Cre $SOCS3^{lox/lox}$ mice with or without LPS injection. We previously reported a significant decrease in the amplitude of both a- and b-waves 24 h after LPS injection in wild-type mice (4). Here, we found that a-wave amplitude, which reflects photoreceptor cell function, had recovered by 10 days after LPS injection in wild-type mice (Fig. 2, F and G). However, the decrease was still measurable in the LPS-administered α -Cre $SOCS3^{lox/lox}$ mice at the same time, suggesting that visual dysfunction has been more profound and prolonged in the SOCS3-deficient mice.

As regards the b-wave, which mainly reflects the function of the inner layers where initial processing and relay of the visual signal from the photoreceptor to the brain are performed, the α -Cre $SOCS3^{lox/lox}$ mice showed a lower amplitude than the wild-type mice both under control conditions and 10 days after LPS injection (Fig. 2I). This may reflect an indirect effect of the

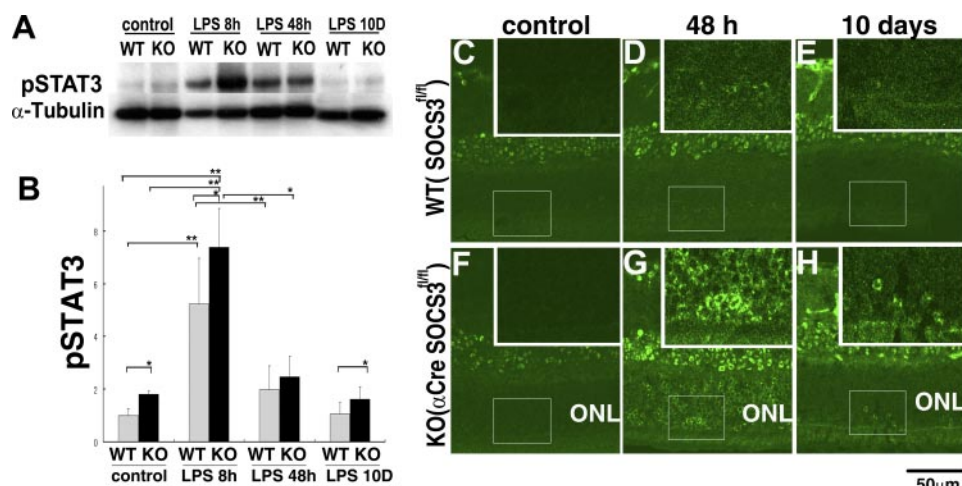


FIGURE 3. STAT3 activation during retinal inflammation was more intensive and prolonged in SOCS3-deficient mice. *A* and *B*, STAT3 activation in wild-type and α -Cre SOCS3^{flx/flx} mice under control conditions and after LPS injection was measured by immunoblot analysis with anti-phospho-STAT3 antibody and normalized to α -tubulin. $n = 5, 5, 7, 7, 5, 4, 5$, and 5 for WT control, KO control, WT 8 h, KO 8 h, WT 48 h, KO 48 h, WT 10 days, and KO 10 days, respectively. *C–H*, STAT3 activation was also analyzed by immunohistochemistry with anti-phospho-STAT3 antibody. The marked areas in the ONL are magnified in insets, *C–H*. Data are expressed as the mean \pm S.D. *, $p < 0.05$; **, $p < 0.01$.

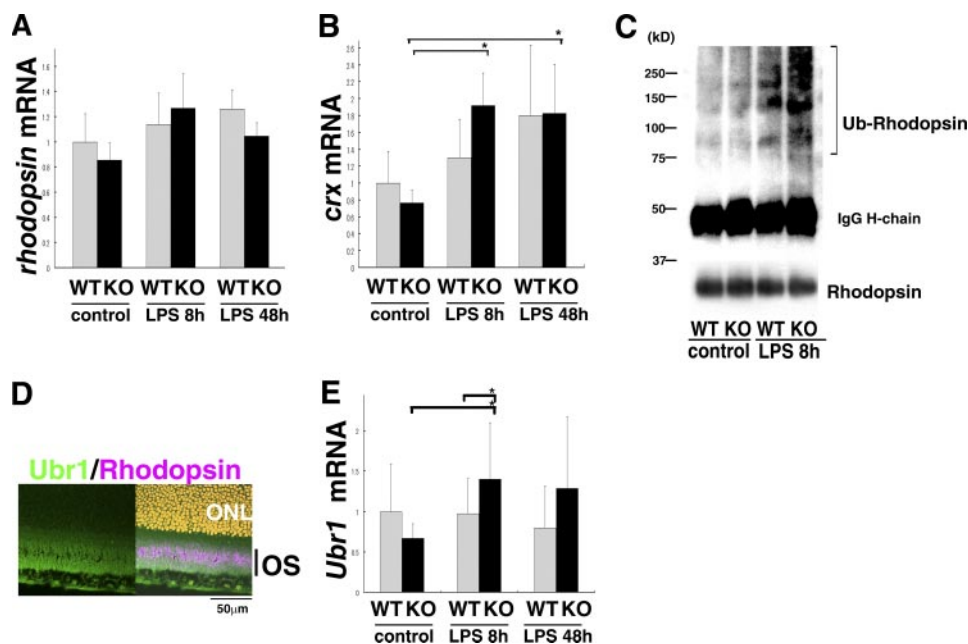


FIGURE 4. Decrease in rhodopsin protein was regulated in a post-transcriptional fashion through degradation by the UPS. *A* and *B*, mRNA levels of *rhodopsin* (*A*) and *crx* (*B*) in the retinas of wild-type and α -Cre SOCS3^{flx/flx} mice under control conditions and after LPS injection were detected by real-time RT-PCR. *C*, retinal lysates from the wild-type and α -Cre SOCS3^{flx/flx} mice under control conditions and 8 h after LPS injection were immunoprecipitated with anti-rhodopsin antibody and then immunoblotted with anti-ubiquitin antibody. Ubiquitin-conjugated rhodopsin protein was observed as a high molecular weight smear. Samples were also immunoblotted with anti-rhodopsin antibody (lower panel). *D*, expression of Ubr1 after LPS injection in the wild-type retina is shown by immunohistochemistry (Ubr1, green; rhodopsin, pink; nuclei counterstained with Hoechst, orange; merged image is shown in the right panel). *E*, mRNA expression of *Ubr1* in the retinas of wild-type and α -Cre SOCS3^{flx/flx} mice under control conditions and after LPS injection were analyzed by real-time RT-PCR. $n = 6, 5, 8, 8, 4$, and 4 for WT control, KO control, WT 8 h, KO 8 h, WT 48 h, and KO 48 h, respectively (*A, B*, and *E*). Data are expressed as the mean \pm S.D. *, $p < 0.05$; Ub-rhodopsin, ubiquitin-conjugated rhodopsin.

photoreceptor cell dysfunction and/or changes in the inner layer during inflammation due to the lack of SOCS3 in the neurites, as well as some developmental disorder caused by the delayed photoreceptor cell differentiation in the α -Cre SOCS3^{flx/flx} mice (10). The implicit time of a- and b- waves showed no differences among the groups (Fig. 2, *H* and *J*).

These results showed that the decrease in rhodopsin after LPS injection, also significant in wild-type mice, was more rapidly and more severely induced in the α -Cre SOCS3^{flx/flx} mice. Consistently, ERG changes induced by retinal inflammation had not recovered even 10 days after LPS injection in the α -Cre SOCS3^{flx/flx} mice. Thus, SOCS3 was required to minimize the changes in the photoreceptor cells during retinal inflammation.

STAT3 Activation Is More Intensive in SOCS3-deficient Mice after LPS Injection—Next, we analyzed whether STAT3 activation was more intensive in the SOCS3-deficient mice and correlated with their more severe rhodopsin reduction. Expectedly, in α -Cre SOCS3^{flx/flx} mice, activated STAT3 was already at a higher level in the whole retina under control conditions as shown by immunoblot analysis (Fig. 3, *A* and *B*), although it was hardly detected immunohistochemically in the photoreceptor cells (Fig. 3, *C* and *F*). The level of activated STAT3 was up-regulated in the retinas of both the wild-type and α -Cre SOCS3^{flx/flx} mice 8 h after LPS injection and was much higher in the α -Cre SOCS3^{flx/flx} mice (Fig. 3, *A* and *B*). Forty-eight hours after LPS injection, although STAT3 activation in the retinas, for the most part, was already down-regulated in both genotypes, activated STAT3 in the ONL was still observed at high levels in most of the photoreceptor cells of the α -Cre SOCS3^{flx/flx} mice (Fig. 3, compare *G* with *D*). This difference of the activated STAT3 levels in the ONL between the both genotypes was not observed under control condition (Fig. 3, compare *F* with *C*). Then, STAT3 activation in the α -Cre SOCS3^{flx/flx} mice gradually diminished but could still be observed clearly in some photoreceptor cells 10 days after LPS injection, in contrast to the wild-type mice (Fig. 3, compare *H* with *E*). Thus, STAT3 activation after LPS injection was more severe and prolonged in the α -Cre SOCS3^{flx/flx} mice.

Rhodopsin Protein Is Down-regulated in a Post-transcriptional Fashion That Involves Degradation through the Ubiquitin

SOCS3 Preserves Rhodopsin Expression and Visual Function

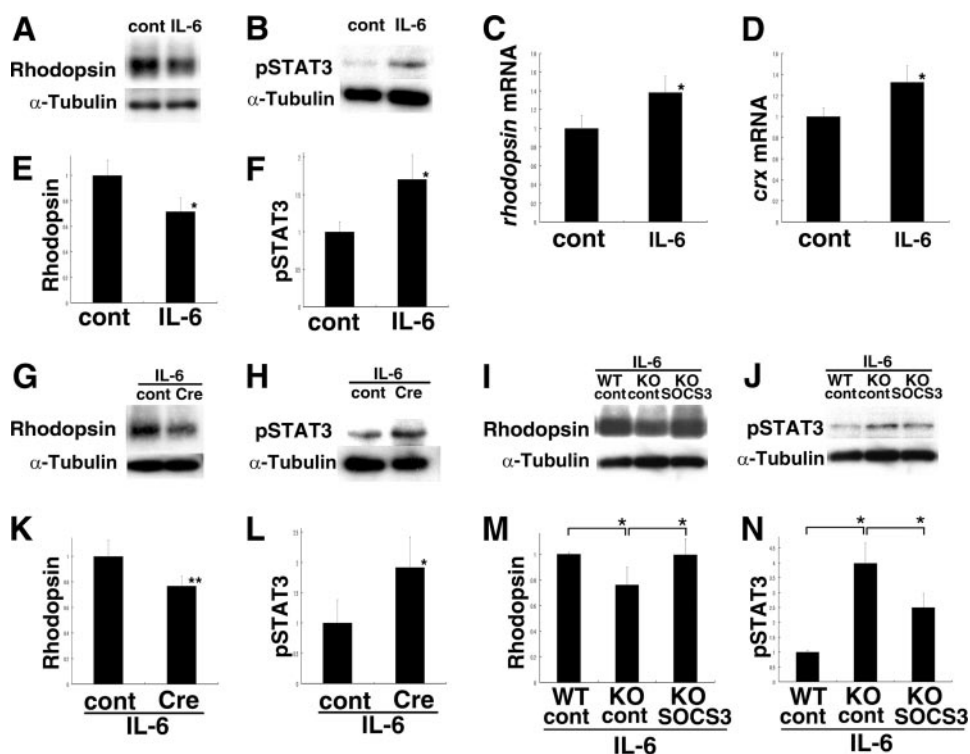


FIGURE 5. Decrease in rhodopsin following IL-6 exposure was exaggerated by SOCS3-deficiency in the adult retinal explants. Adult retinal explants were exposed to IL-6 (10 ng/ml) for 4 h. Levels of rhodopsin protein (A and E) and STAT3 activation (B and F) were measured by immunoblot analyses. mRNA expression of *rhodopsin* (C) and *crx* (D) were analyzed by real-time RT-PCR. Adult retinal explants derived from SOCS3 floxed mice were electroporated with plasmid CAG-Cre or pCAG-control (G, H, K, and L), and adult retinal explants derived from α -Cre SOCS3^{fllox/fllox} mice were introduced with pCAG-control or pCAG-SOCS3 (I, J, M, and N); all were exposed to IL-6 for 4 h. Levels of rhodopsin protein (G, I, K, and M) and STAT3 activation (H, J, L, and N) were measured by immunoblot analyses. Bands of rhodopsin appeared to represent monomers based on their electrophoretic mobility. *n* = 4. Data are expressed as the mean \pm S.D. *, *p* < 0.05; **, *p* < 0.01.

ubitin-Proteasome System—Interestingly, mRNA expression of both *rhodopsin* and *crx* was not down-regulated (Fig. 4, A and B), actually *crx* was up-regulated after LPS injection, although the rhodopsin protein level dropped (Fig. 2, A and D). Therefore, rhodopsin reduction during inflammation in adults was under post-transcriptional inhibition, which is different from the mechanism that inhibits rhodopsin expression in embryos (8, 10). Nevertheless, SOCS3 was required to suppress the decrease in rhodopsin in both cases.

Under stress conditions, bulk protein degradation through the UPS increases (33). The fact that the decrease in rhodopsin protein levels during inflammation was rapid supported the idea that enhanced degradation of the rhodopsin protein through the UPS was responsible. To investigate whether ubiquitin-conjugated rhodopsin is up-regulated during retinal inflammation, retinal cell lysates were subjected to immunoprecipitation with an anti-rhodopsin antibody followed by immunoblotting with an anti-ubiquitin antibody. Under normal conditions, the level of ubiquitin-conjugated rhodopsin was about the same in the retinas of both wild-type and α -Cre SOCS3^{fllox/fllox} mice (Fig. 4C). However, 8 h after LPS injection, the level of ubiquitin-conjugated rhodopsin protein, shown as a high molecular weight smear, was up-regulated in the retinas of both genotypes. This effect was more marked in the α -Cre

SOCS3^{fllox/fllox} retina (Fig. 4C), suggesting an involvement of UPS in rhodopsin reduction and a link between STAT3 activation and the ubiquitin conjugation of rhodopsin.

Furthermore, we found that a probable E3 ubiquitin ligase for rhodopsin degradation, ubiquitin-protein ligase E3 component, *n*-recogin 1 (Ubr1) (as described under “Discussion”), was expressed in the OS in the inflamed retina (Fig. 4D). *Ubr1* mRNA expression, which is known to be dependent on STAT3 activity (34), was analyzed by real-time RT-PCR and found to be up-regulated 8 h after LPS injection in the α -Cre SOCS3^{fllox/fllox} retinas (Fig. 4E). This result supported the idea that the decrease in rhodopsin through the UPS was linked to STAT3 activation. Thus, rhodopsin protein levels were post-transcriptionally inhibited during retinal inflammation, at least in part by degradation through the UPS.

SOCS3 Preserves Rhodopsin and Inhibits STAT3 Activation following IL-6 Exposure in Adult Retinal Explants—To investigate the mechanism of decrease in rhodopsin during inflammation, we utilized retinal explants derived from adult retinas (adult retinal explants). One

of the inflammatory cytokines and upstream of STAT3 activation, IL-6 is known to be up-regulated during LPS-induced inflammation (2, 3, 25–27). Although several kinds of cytokines should influence retinal cells during inflammation, we exposed adult retinal explants to IL-6 for 4 h to activate STAT3 and examined the levels of rhodopsin. In this system as well, rhodopsin protein decreased (Fig. 5, A and E), and STAT3 was activated (Fig. 5, B and F). The mRNA levels of *rhodopsin* and *crx* were not decreased by exposure to IL-6 (Fig. 5, C and D). Thus, rhodopsin levels reduced post-transcriptionally as also found *in vivo*. Although IL-6 may not be the only cytokine that activates STAT3 during inflammation, exposure to IL-6, at least in part, led to a retinal condition that mimicked inflammation.

Using this system, we first investigated whether SOCS3 was directly responsible for the severe decrease in rhodopsin protein in the α -Cre SOCS3^{fllox/fllox} mice during retinal inflammation, because the decrease might have been due to secondary changes in the mutant mice. To down-regulate SOCS3 experimentally in adult retinal explants from SOCS3^{fllox/fllox} mice with no Cre transgene, the explants were electroporated to introduce a Cre expression vector plasmid (pCAG-Cre) or an empty vector (pCAG-control, as a control) and exposed to IL-6. The residual levels of rhodopsin

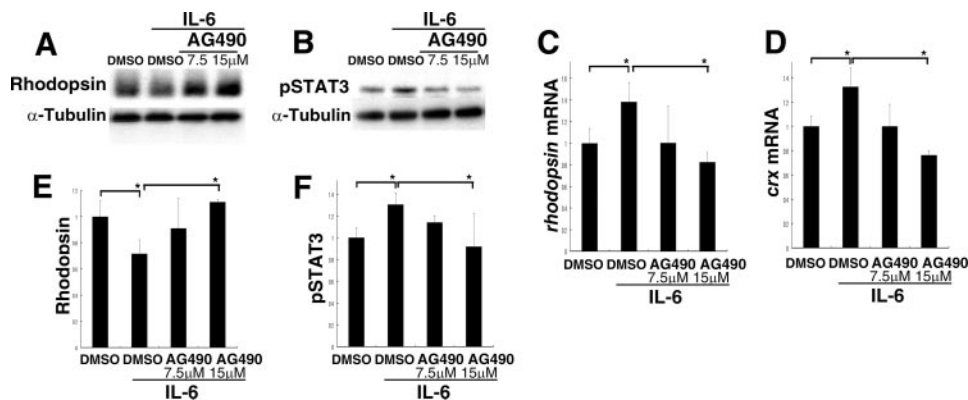


FIGURE 6. Decrease in rhodopsin following IL-6 exposure was regulated by STAT3 activation in a post-transcriptional fashion. A–F, adult wild-type retinal explants were cultured under IL-6 exposure with or without a JAK inhibitor, AG490 (diluted in DMSO in 7.5 or 15 μM). Immunoblot analyses show levels of rhodopsin protein (A and E) and STAT3 activation (B and F) after exposure to IL-6. mRNA levels of *rhodopsin* (C) and *crx* (D) were measured by real-time RT-PCR. For control, DMSO was added. Data are expressed as the mean ± S.D. (n = 3). *, p < 0.05.

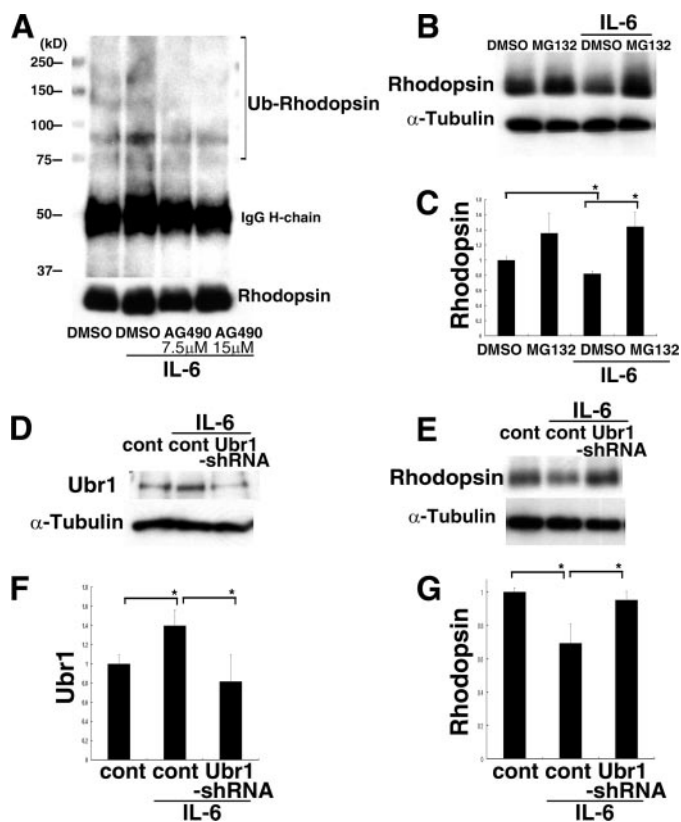


FIGURE 7. Rhodopsin protein was degraded through the UPS by Ubr1 after IL-6 exposure. A, retinal cell lysates from adult retinal explants derived from α -Cre *SOCS3^{flax/flax}* mice exposed to IL-6, with or without AG490, for 30 min were immunoprecipitated with anti-rhodopsin antibody and then immunoblotted with anti-ubiquitin antibody. Ubiquitin-conjugated rhodopsin was shown as a high molecular weight smear. Samples were also immunoblotted with anti-rhodopsin antibody (lower panel). B and C, adult retinal explants derived from α -Cre *SOCS3^{flax/flax}* mice were cultured with or without IL-6 and a proteasome inhibitor, MG132, for 4 h, and the rhodopsin protein level was measured by immunoblot analysis. D–G, adult wild-type retinal explants infected with a lentivirus carrying a specific shRNA to knock down Ubr1 were exposed to IL-6 for 4 h. Ubr1 expression (D and F) and rhodopsin protein levels (E and G) were analyzed by immunoblot analyses. Data are expressed as the mean ± S.D. (n = 4). *, p < 0.05. Ub-rhodopsin, ubiquitin-conjugated rhodopsin.

after IL-6 exposure were lower (Fig. 5, G and K) and those of activated STAT3 were higher (Fig. 5, H and L) after pCAG-Cre introduction.

Next, we introduced a SOCS3 expression vector (pCAG-SOCS3) or an empty vector (pCAG-control) into adult retinal explants derived from α -Cre *SOCS3^{flax/flax}* mice. The SOCS3-deficient retinal explants showed much less rhodopsin expression after IL-6 exposure than the wild-type retinal explants, the same as found *in vivo*; however, this decrease was cancelled by the introduction of pCAG-SOCS3 (Fig. 5, I and M). As expected, STAT3 activation up-regulated in the *SOCS3*-deficient adult retinal explants was clearly down-regulated after the introduction of pCAG-SOCS3 (Fig. 5, J and N). These data indicated

that the *SOCS3* deficiency itself was responsible for the decrease in rhodopsin that followed exposure to IL-6/gp130 signals in the adult retina.

Rhodopsin Is Regulated by Activated STAT3 at the Post-transcriptional Level after IL-6 Exposure—The levels of rhodopsin correlated negatively with STAT3 activation in all cases tested both *in vivo* and *in vitro*. We therefore analyzed whether STAT3 activation reduced the expression of the rhodopsin protein. A JAK inhibitor, AG490, which inhibits STAT3 activation, suppressed the decrease in rhodopsin protein level after IL-6 exposure in adult wild-type retinal explants (Fig. 6, A and E) concomitant with a dose-dependent decrease in activated STAT3 (Fig. 6, B and F). Further evidence of the role of activated STAT3 was obtained by introducing a plasmid encoding a dominant-negative form of STAT3, pCAG-STAT3F (35, 36), into adult retinal explants before exposure to IL-6. The pCAG-STAT3F expression reduced the level of activated STAT3 and increased the amount of residual rhodopsin protein (data not shown). In contrast, an inhibitor of ERK, U0126 (20 μM), which down-regulated ERK activity in the adult retinal explants, did not avoid rhodopsin reduction by IL-6 (data not shown), confirming that activation of ERK, another downstream pathway of gp130 signaling, was not responsible for the decrease in rhodopsin.

Moreover, transcription of *rhodopsin* and *crx* was not inhibited but rather up-regulated after STAT3 activation (Fig. 6, C and D). Thus, the reduction in rhodopsin protein levels by activated STAT3 was caused by a post-transcriptional mechanism.

Rhodopsin Protein Is Degraded through UPS after IL-6 Exposure—Next, we examined whether UPS was involved in the STAT3-dependent decrease in rhodopsin in the adult retinal explants. For this purpose, we analyzed ubiquitin-conjugated rhodopsin in the extract from the adult retinal explants 30 min after IL-6 exposure with or without AG490. α -Cre *SOCS3^{flax/flax}* adult retinal explants, in which STAT3 can be activated intensively, were utilized, and the extract was processed into immunoprecipitation with anti-rhodopsin antibody. Ubiquitin-conjugated rhodopsin was clearly detected as a high molecular weight smear and up-regulated after IL-6 exposure. This was suppressed by AG490 treatment, which inhibits

SOCS3 Preserves Rhodopsin Expression and Visual Function

STAT3 activation (Fig. 7A), suggesting that STAT3 activation contributes to the degradation of rhodopsin through the UPS. Furthermore, a proteasome inhibitor, MG132, reversed the level of rhodopsin after IL-6 exposure in the α -Cre *SOCS3^{fllox/fllox}* adult retinal explants (Fig. 7, B and C). This confirmed that the UPS was involved in the decrease in rhodopsin by an inflammatory cytokine, IL-6. The fact that MG132 also tended to increase rhodopsin protein level in the absence of IL-6 exposure can be explained by the originally higher levels of STAT3 activation in the α -Cre *SOCS3^{fllox/fllox}* adult retinal explants.

Then, we also examined whether an E3 ubiquitin ligase, Ubr1, was involved in this regulation. Adult wild-type retinal explants, infected with a lentivirus carrying a specific shRNA to knock down Ubr1, were exposed to IL-6. We first confirmed that Ubr1 induced by IL-6 was successfully down-regulated by the Ubr1 shRNA (Fig. 7, D and F). Interestingly, a decrease in rhodopsin after IL-6 exposure was avoided by suppression of Ubr1 (Fig. 7, E and G). These data thus indicate that highly activated STAT3 after IL-6 exposure induced Ubr1 and UPS to degrade rhodopsin.

DISCUSSION

The present data have demonstrated that SOCS3 protects photoreceptor cells from severe down-regulation of rhodopsin protein and prolonged visual dysfunction during retinal inflammation. Elevated STAT3 activation decreased rhodopsin at the post-transcriptional level through degradation by the UPS. SOCS3 effectively inhibited STAT3 activation and blocked further photoreceptor cell dysfunction.

SOCS3 Minimizes Visual Dysfunction during Retinal Inflammation—We demonstrated that STAT3 activation, among several intracellular signaling pathways induced during retinal inflammation, was critical for visual function and that SOCS3 was a key endogenous molecule for neuroprotection. Although rhodopsin expression was also significantly down-regulated in wild-type mice when STAT3 activation reached a certain level, this change was more rapid and profound in α -Cre *SOCS3^{fllox/fllox}* mice (Fig. 2, A and D), indicating that SOCS3 was required to minimize and recover from the retinal dysfunction. This also suggested that *SOCS3* deficiency compromised the ability of their photoreceptor cells to withstand inflammatory stress. SOCS3 may have an important role in balancing STAT3 activation during fluctuations of the microenvironment in daily life, and by so doing, SOCS3 may help avoid the development of severe inflammation.

Rhodopsin expression was better preserved, but still reduced, in the wild-type mice during the course of inflammation. This is more likely because the level of SOCS3 expression is not sufficient to significantly suppress the active phosphorylation of STAT3 by JAK, which had been induced by the strong inflammatory stimuli, even though the SOCS3 expression is induced. Although exposure to IL-6 alone reduced rhodopsin in adult retinal explants, several kinds of inflammatory cytokines that activate STAT3 more intensively *in vivo* should be induced simultaneously during inflammation. The level of SOCS3 is itself regulated by several kinds of post-transcriptional inhibitory mechanisms (10, 25, 37), which may also cause the insufficiency under high levels of STAT3 activation. The

inadequate SOCS3 activity may cause visual dysfunction also in other situations. STAT3 activation induced by CNTF administration for therapy in retinitis pigmentosa may easily exceed the activity of endogenous SOCS3 and induce excessive STAT3 activation. Other examples are retinal degeneration and light damage (38), which also up-regulates CNTF/gp130-STAT3 signaling in the retina. In these retinas, rhodopsin degradation may be accelerated, causing increased deterioration of retinal function when STAT3 activation surpasses endogenous SOCS3 activity. As several kinds of cytokine signals that activate STAT3 are up-regulated during inflammation, it would be a great advantage for SOCS3 to simultaneously shut down several of the pathologic signaling pathways by directly inhibiting JAK, commonly found downstream of the gp130 signals, as compared with the strategy designed to entrap each cytokine. Further study may support the development of the SOCS3 protein as a therapeutic target (2, 39).

Proposed Mechanism for SOCS3 to Inhibit the UPS-dependent Degradation of Rhodopsin—The rapid decrease in rhodopsin protein at least in part involved UPS-mediated degradation. Although rhodopsin is not metabolized through the UPS under normal condition (40), it can be degraded rapidly through the UPS under pathologic conditions (41).

A mutant rhodopsin, P23H, which causes an autosomal dominant form of retinitis pigmentosa, folds abnormally and accumulates in aggresomes instead of proceeding to the normal transport to the cell membrane (41, 42). However, the wild-type rhodopsin protein was also ubiquitinated (Figs. 4C and 7), suggesting that a normal rhodopsin protein may undergo abnormal post-translational modification and misfolding, which leads to degradation by the UPS in response to stress stimuli. Ubiquitin protein is already present in the rod outer segment under control conditions (43), and thus it may lead rhodopsin protein degraded so rapidly. The authors (43) also showed that rhodopsin and ubiquitin proteins are both observed in the same vesicles especially after light exposure, supporting the idea that genetically normal rhodopsin may be degraded through the UPS under pathological conditions.

Activated STAT3 regulated multi-ubiquitination (Fig. 7A). Thus, we deduced Ubr1 as a selective E3 ubiquitin ligase for rhodopsin degradation as follows. An ubiquitin-conjugating enzyme, E2_{14k}, required for “N-end rule” proteolysis, is abundant in the fraction of rod outer segments as well as rhodopsin (40). E2_{14k}, which is indispensable for the catabolism of skeletal muscle during fasting, interacts with a selective E₃ ubiquitin ligase, Ubr1 (33). Because an E2 and E3 enzymes act with a particular combination to degrade specific target proteins, E2_{14k} and Ubr1 could be involved in the selective degradation of rhodopsin protein observed in this study. Interestingly, Ubr1 expression is dependent on the STAT3 activity induced by the IL-6/gp130 signaling pathway (34). We found that Ubr1 was expressed in the OS of the photoreceptor cells, which encouraged us to further pursue the responsibility of Ubr1 for rhodopsin degradation following IL-6 exposure (Fig. 7, D–G). Moreover, *Ubr1* mRNA expression was significantly up-regulated after LPS injection in the retinas of α -Cre *SOCS3^{fllox/fllox}* mice, where STAT3 activation was exaggerated. Thus, SOCS3 may contribute to photoreceptor cell protection during retinal inflamma-

tion by inhibiting the expression of the UPS-related gene, *Ubr1*, through suppression of STAT3 activation. This suggests that *Ubr1* may also be a therapeutic target during retinal inflammation.

An alternative role of STAT3 activation on accelerating UPS may be as follows. Polarized microtubules, which promote the accumulation of misfolded proteins into aggresomes (44), are stabilized by STAT3 activation (45). Therefore, the intracellular conditions during inflammation would promote the aggregation of misfolded rhodopsin.

In addition to direct induction of the UPS, some other mechanisms could be involved in the post-transcriptional inhibition of rhodopsin expression. SOCS3 was expressed not only in photoreceptor cells but also in Müller glial cells during inflammation. It is possible that excessive STAT3 activation could induce the release of cytokines by the Müller glial cells that secondarily up-regulated the UPS and/or other post-transcriptional mechanisms in the photoreceptor cells, especially in those of the α -Cre *SOCS3^{flox/flox}* mice. Otherwise, expression of rhodopsin kinase, which is involved in rhodopsin turnover under normal conditions (46), was up-regulated 8 h after LPS injection in α -Cre *SOCS3^{flox/flox}* mice, although its level trended downward at 48 h following the decrease in rhodopsin (data not shown). Therefore, up-regulation of the general pathway for rhodopsin degradation could also contribute to its reduced levels (12). In LPS-induced retinal inflammation, various kinds of cytokines could also be involved, causing either cell-autonomous or non-cell-autonomous effects on rhodopsin expression with or without STAT3-dependent mechanism. Further investigation should be continued to clarify the detailed mechanisms.

Distinct Regulation of Rhodopsin Expression between the Developing and Adult Retina—We reported previously that STAT3 activation inhibits rhodopsin expression at transcriptional levels in the developing retina. SOCS3 is required to initiate the transcription of *rhodopsin* and *crx*, inhibiting STAT3 activation in the perinatal period (10). This situation resembles that in the adult retina during inflammation. However, unexpectedly, the amounts of *rhodopsin* and *crx* transcripts did not decrease with STAT3 activation during inflammation or after IL-6 exposure. These results suggest that the underlying mechanisms for regulating the transcription and/or RNA stability of *rhodopsin* and *crx* are different in the inflamed adult retina than in the developing retina (8, 10). One explanation for this finding is that rhodopsin is a part of a negative feedback loop controlling its own transcription, and the loss of rhodopsin protein therefore rather induces the mRNAs, even in the presence of high levels of STAT3 activation. This is consistent with the fact that the level of *crx* mRNA increases with new rhodopsin production during development and then is somewhat down-regulated after rhodopsin reaches its plateau level (47, 48). Alternatively, the effect of STAT3 activation in the surrounding retinal cells, such as Müller glial cells, rather than a direct action in photoreceptor cells, may be one of the pathways for the present observation.

As regards transcription under normal condition, the same mechanism as in the developing retina may be also applicable in the adult, since mRNA expression of *rhodopsin* and *crx* tended to be down-regulated in α -Cre *SOCS3^{flox/flox}* mice in which

STAT3 is more activated. But redundant regulatory mechanisms should be present given that rhodopsin protein levels in the α -Cre *SOCS3^{flox/flox}* mice caught up with those in wild-type mice and the a-wave in ERG was normal in the adult mutants.

Therefore, rhodopsin protein was down-regulated in a post-transcriptional fashion, which involves protein degradation through the UPS, most probably activated by STAT3-dependent E3 ubiquitin ligase, *Ubr1*. SOCS3 minimizes and promotes recovery from this influence of inflammatory signaling by inhibiting STAT3 activation, thereby contributing to the preservation of rhodopsin expression and visual function.

Acknowledgments—We are very grateful to Dr. Peter Gruss for providing α -Cre transgenic mice, Dr. Jun-ichi Miyazaki for CAG-CAT-EGFP transgenic mice, and Dr. Hitoshi Niwa for the plasmid CAG. We also thank Haruna Koizumi for technical assistance and Dr. Hirobumi Tada for technical advice concerning these experiments.

REFERENCES

1. Suzuki, K., Yoshimura, Y., Hisada, Y., and Matsumoto, A. (1994) *Jpn. J. Pharmacol.* **64**, 97–102
2. Shouda, T., Yoshida, T., Hanada, T., Wakioka, T., Oishi, M., Miyoshi, K., Komiya, S., Kosai, K., Hanakawa, Y., Hashimoto, K., Nagata, K., and Yoshimura, A. (2001) *J. Clin. Invest.* **108**, 1781–1788
3. Nagai, N., Oike, Y., Noda, K., Urano, T., Kubota, Y., Ozawa, Y., Shinoda, H., Koto, T., Shinoda, K., Inoue, M., Tsubota, K., Yamashiro, K., Suda, T., and Ishida, S. (2005) *Investig. Ophthalmol. Vis. Sci.* **46**, 2925–2931
4. Kurihara, T., Ozawa, Y., Shinoda, K., Nagai, N., Inoue, M., Oike, Y., Tsubota, K., Ishida, S., and Okano, H. (2006) *Investig. Ophthalmol. Vis. Sci.* **47**, 5545–5552
5. Ezzeddine, Z. D., Yang, X., DeChiara, T., Yancopoulos, G., and Cepko, C. L. (1997) *Development (Camb.)* **124**, 1055–1067
6. Neophytou, C., Vernallis, A. B., Smith, A., and Raff, M. C. (1997) *Development (Camb.)* **124**, 2345–2354
7. Schulz-Key, S., Hofmann, H. D., Beisenherz-Huss, C., Barbisch, C., and Kirsch, M. (2002) *Investig. Ophthalmol. Vis. Sci.* **43**, 3099–3108
8. Ozawa, Y., Nakao, K., Shimazaki, T., Takeda, J., Akira, S., Ishihara, K., Hirano, T., Oguchi, Y., and Okano, H. (2004) *Mol. Cell. Neurosci.* **26**, 258–270
9. Rhee, K. D., Goureau, O., Chen, S., and Yang, X. J. (2004) *J. Neurosci.* **24**, 9779–9788
10. Ozawa, Y., Nakao, K., Shimazaki, T., Shimmura, S., Kurihara, T., Ishida, S., Yoshimura, A., Tsubota, K., and Okano, H. (2007) *Dev. Biol.* **303**, 591–600
11. Rhee, K. D., Ruiz, A., Duncan, J. L., Hauswirth, W. W., Lavail, M. M., Bok, D., and Yang, X. J. (2007) *Investig. Ophthalmol. Vis. Sci.* **48**, 1389–1400
12. Wen, R., Song, Y., Kjellstrom, S., Tanikawa, A., Liu, Y., Li, Y., Zhao, L., Bush, R. A., Laties, A. M., and Sieving, P. A. (2006) *J. Neurosci.* **26**, 13523–13530
13. Sieving, P. A., Caruso, R. C., Tao, W., Coleman, H. R., Thompson, D. J., Fullmer, K. R., and Bush, R. A. (2006) *Proc. Natl. Acad. Sci. U. S. A.* **103**, 3896–3901
14. Mori, H., Hanada, R., Hanada, T., Aki, D., Mashima, R., Nishinakamura, H., Torisu, T., Chien, K. R., Yasukawa, H., and Yoshimura, A. (2004) *Nat. Med.* **10**, 739–743
15. Marquardt, T., Ashery-Padan, R., Andrejewski, N., Scardigli, R., Guillemot, F., and Gruss, P. (2001) *Cell* **105**, 43–55
16. Niwa, H., Yamamura, K., and Miyazaki, J. (1991) *Gene* **108**, 193–199
17. Tomita, K., Ishibashi, M., Nakahara, K., Ang, S. L., Nakanishi, S., Guillemot, F., and Kageyama, R. (1996) *Neuron* **16**, 723–734
18. Hanada, T., Yoshida, T., Kinjyo, I., Minoguchi, S., Yasukawa, H., Kato, S., Mimata, H., Nomura, Y., Seki, Y., Kubo, M., and Yoshimura, A. (2001) *J. Biol. Chem.* **276**, 40746–40754
19. Suzuki, A., Hanada, T., Mitsuyama, K., Yoshida, T., Kamizono, S., Hoshino, T., Kubo, M., Yamashita, A., Okabe, M., Takeda, K., Akira, S.,

SOCS3 Preserves Rhodopsin Expression and Visual Function

- Matsumoto, S., Toyonaga, A., Sata, M., and Yoshimura, A. (2001) *J. Exp. Med.* **193**, 471–481
20. Sasaki, A., Inagaki-Ohara, K., Yoshida, T., Yamanaka, A., Sasaki, M., Yasukawa, H., Koromilas, A. E., and Yoshimura, A. (2003) *J. Biol. Chem.* **278**, 2432–2436
21. Furukawa, T., Morrow, E. M., Li, T., Davis, F. C., and Cepko, C. L. (1999) *Nat. Genet.* **23**, 466–470
22. Peng, G. H., Ahmad, O., Ahmad, F., Liu, J., and Chen, S. (2005) *Hum. Mol. Genet.* **14**, 747–764
23. Kurihara, T., Ozawa, Y., Nagai, N., Shinoda, K., Noda, K., Imamura, Y., Tsubota, K., Okano, H., Oike, Y., and Ishida, S. (2008) *Diabetes*, in press
24. Koizumi, K., Poulaki, V., Doehmen, S., Welsandt, G., Radetzky, S., Lapps, A., Kociok, N., Kirchof, B., and Joussen, A. M. (2003) *Investig. Ophthalmol. Vis. Sci.* **44**, 2184–2191
25. Yasukawa, H., Ohishi, M., Mori, H., Murakami, M., Chinen, T., Aki, D., Hanada, T., Takeda, K., Akira, S., Hoshijima, M., Hirano, T., Chien, K. R., and Yoshimura, A. (2003) *Nat. Immunol.* **4**, 551–556
26. Yang, X. P., Schaper, F., Teubner, A., Lammert, F., Heinrich, P. C., Matern, S., and Siewert, E. (2005) *J. Hepatol.* **43**, 704–710
27. Lebel, E., Vallieres, L., and Rivest, S. (2000) *Endocrinology* **141**, 3749–3763
28. Okada, S., Nakamura, M., Katoh, H., Miyao, T., Shimazaki, T., Ishii, K., Yamane, J., Yoshimura, A., Iwamoto, Y., Toyama, Y., and Okano, H. (2006) *Nat. Med.* **12**, 829–834
29. Reich, N. C., and Liu, L. (2006) *Nat. Rev. Immunol.* **6**, 602–612
30. Shah, M., Patel, K., Mukhopadhyay, S., Xu, F., Guo, G., and Sehgal, P. B. (2006) *J. Biol. Chem.* **281**, 7302–7308
31. Ndubuisi, M. I., Guo, G. G., Fried, V. A., Etlinger, J. D., and Sehgal, P. B. (1999) *J. Biol. Chem.* **274**, 25499–25509
32. Roberts, A. W., Robb, L., Rakar, S., Hartley, L., Cluse, L., Nicola, N. A., Metcalf, D., Hilton, D. J., and Alexander, W. S. (2001) *Proc. Natl. Acad. Sci. U. S. A.* **98**, 9324–9329
33. Adegoke, O. A., Bedard, N., Roest, H. P., and Wing, S. S. (2002) *Am. J. Physiol.* **283**, E482–E489
34. Sasaki, T., Kojima, H., Kishimoto, R., Ikeda, A., Kunimoto, H., and Nakajima, K. (2006) *Mol. Cell* **24**, 63–75
35. Nakajima, K., Yamanaka, Y., Nakae, K., Kojima, H., Ichiba, M., Kiuchi, N., Kitaoka, T., Fukada, T., Hibi, M., and Hirano, T. (1996) *EMBO J.* **15**, 3651–3658
36. Minami, M., Inoue, M., Wei, S., Takeda, K., Matsumoto, M., Kishimoto, T., and Akira, S. (1996) *Proc. Natl. Acad. Sci. U. S. A.* **93**, 3963–3966
37. Babon, J. J., McManus, E. J., Yao, S., DeSouza, D. P., Mielke, L. A., Sprigg, N. S., Willson, T. A., Hilton, D. J., Nicola, N. A., Baca, M., Nicholson, S. E., and Norton, R. S. (2006) *Mol. Cell* **22**, 205–216
38. Samardzija, M., Wenzel, A., Aufenberg, S., Thiersch, M., Reme, C., and Grimm, C. (2006) *FASEB J.* **20**, 2411–2413
39. Jo, D., Liu, D., Yao, S., Collins, R. D., and Hawiger, J. (2005) *Nat. Med.* **11**, 892–898
40. Obin, M. S., Jahngen-Hodge, J., Nowell, T., and Taylor, A. (1996) *J. Biol. Chem.* **271**, 14473–14484
41. Illing, M. E., Rajan, R. S., Bence, N. F., and Kopito, R. R. (2002) *J. Biol. Chem.* **277**, 34150–34160
42. Saliba, R. S., Munro, P. M., Luthert, P. J., and Cheetham, M. E. (2002) *J. Cell Sci.* **115**, 2907–2918
43. Reme, C. E., Wolfrum, U., Imsand, C., Hafezi, F., and Williams, T. P. (1999) *Investig. Ophthalmol. Vis. Sci.* **40**, 2398–2404
44. Kopito, R. R. (2000) *Trends Cell Biol.* **10**, 524–530
45. Ng, D. C., Lin, B. H., Lim, C. P., Huang, G., Zhang, T., Poli, V., and Cao, X. (2006) *J. Cell Biol.* **172**, 245–257
46. Stryer, L. (1991) *J. Biol. Chem.* **266**, 10711–10714
47. Furukawa, A., Koike, C., Lippincott, P., Cepko, C. L., and Furukawa, T. (2002) *J. Neurosci.* **22**, 1640–1647
48. Furukawa, T., Morrow, E. M., and Cepko, C. L. (1997) *Cell* **91**, 531–541